Plant Physiol. (1998) 117: 545–557

Strontium-Induced Repetitive Calcium Spikes in a Unicellular Green Alga[1]

Claudia S. Bauer, Christoph Plieth[2], Birgit Bethmann, Ondina Popescu[3], Ulf-Peter Hansen, Wilhelm Simonis, and Gerald Schönknecht*

Botany I, University of Würzburg, Julius-von-Sachs Platz 2, D-97082 Würzburg, Germany (C.S.B., B.B., O.P., W.S., G.S.); and Institute for Applied Physics, University of Kiel, Olshausenstrasse 40, D-24098 Kiel, Germany (C.P., U.-P.H.)

The divalent cation Sr^{2+} induced repetitive transient spikes of the cytosolic Ca^{2+} activity $[Ca^{2+}]_{cy}$ and parallel repetitive transient hyperpolarizations of the plasma membrane in the unicellular green alga *Eremosphaera viridis*. $[Ca^{2+}]_{cy}$ measurements, membrane potential measurements, and cation analysis of the cells were used to elucidate the mechanism of Sr^{2+}-induced $[Ca^{2+}]_{cy}$ oscillations. Sr^{2+} was effectively and rapidly compartmentalized within the cell, probably into the vacuole. The $[Ca^{2+}]_{cy}$ oscillations cause membrane potential oscillations, and not the reverse. The endoplasmic reticulum (ER) Ca^{2+}-ATPase blockers 2,5-di-tert-butylhydroquinone and cyclopiazonic acid inhibited Sr^{2+}-induced repetitive $[Ca^{2+}]_{cy}$ spikes, whereas the compartmentalization of Sr^{2+} was not influenced. A repetitive Ca^{2+} release and Ca^{2+} re-uptake by the ER probably generated repetitive $[Ca^{2+}]_{cy}$ spikes in *E. viridis* in the presence of Sr^{2+}. The inhibitory effect of ruthenium red and ryanodine indicated that the Sr^{2+}-induced Ca^{2+} release from the ER was mediated by a ryanodine/cyclic ADP-ribose type of Ca^{2+} channel. The blockage of Sr^{2+}-induced repetitive $[Ca^{2+}]_{cy}$ spikes by La^{3+} or Gd^{3+} indicated the necessity of a certain influx of divalent cations for sustained $[Ca^{2+}]_{cy}$ oscillations. Based on these data we present a mathematical model that describes the baseline spiking $[Ca^{2+}]_{cy}$ oscillations in *E. viridis*.

Transient elevations of the $[Ca^{2+}]_{cy}$ play a central role in intracellular signal transduction in plant (Bush, 1995; Trewavas et al., 1996; Webb et al., 1996) and animal cells (Petersen et al., 1994; Bootman and Berridge, 1995). Brief transient $[Ca^{2+}]_{cy}$ elevations with a rapid rising phase and a rapid falling phase are called $[Ca^{2+}]_{cy}$ spikes, reflecting the shape of these $[Ca^{2+}]_{cy}$ transients. Single $[Ca^{2+}]_{cy}$ spikes can be induced by mechanical signals, cold shock, or elicitors in plant cells. A correlation between mechanical signal strength and amplitude of the resulting $[Ca^{2+}]_{cy}$ spike has been shown (Knight et al., 1991, 1992), suggesting a role of $[Ca^{2+}]_{cy}$ spikes in signal transduction in plant cells. In animal cells repetitive transient elevations of $[Ca^{2+}]_{cy}$, so-called $[Ca^{2+}]_{cy}$ oscillations, are well established (Tsien and Tsien, 1990; Fewtrell, 1993; Petersen et al., 1994). For plant cells only a few reports about $[Ca^{2+}]_{cy}$ oscillations exist. Phytohormone-induced $[Ca^{2+}]_{cy}$ fluctuations reported earlier were strongly damped and ceased after a few repetitions (Felle, 1988; Schroeder and Hagiwara, 1990). Only recently stable $[Ca^{2+}]_{cy}$ oscillations were observed in plant cells (Johnson et al., 1995; McAinsh et al., 1995; Ehrhardt et al., 1996; Bauer et al., 1997). In some cases these $[Ca^{2+}]_{cy}$ oscillations display a baseline spiking pattern, which means that repetitive $[Ca^{2+}]_{cy}$ spikes are separated by a constant $[Ca^{2+}]_{cy}$ baseline (Ehrhardt et al., 1996; Bauer et al., 1997). There are indications for a physiological function of $[Ca^{2+}]_{cy}$ oscillations in plant cells (Johnson et al., 1995; McAinsh et al., 1995; Ehrhardt et al., 1996). The mechanisms generating $[Ca^{2+}]_{cy}$ oscillations in plant cells are unknown.

The unicellular green alga *Eremosphaera viridis* responds to various stimuli with single or repetitive $[Ca^{2+}]_{cy}$ spikes (Bauer et al., 1997). For example, after a "light-off" stimulus a single $[Ca^{2+}]_{cy}$ spike occurs, which is accompanied by a parallel transient hyperpolarization of the plasma membrane. The addition of caffeine or Sr^{2+} induces repetitive $[Ca^{2+}]_{cy}$ spikes that are always accompanied by repetitive transient hyperpolarizations. This hyperpolarization of the plasma membrane is due to the opening of Ca^{2+}-dependent K^+ channels (Thaler et al., 1989; Förster, 1990), representing a qualitative indicator of $[Ca^{2+}]_{cy}$ spikes (Bauer et al., 1997). In this study the long-lasting Sr^{2+}-induced repetitive $[Ca^{2+}]_{cy}$ spikes in *E. viridis* were used to elucidate the mechanism of $[Ca^{2+}]_{cy}$ oscillations in a green plant cell. We developed a theoretical model that serves as a basis to discuss which intracellular Ca^{2+} stores might be involved in generating $[Ca^{2+}]_{cy}$ spikes.

[1] This work was financially supported by the Deutsche Forschungsgemeinschaft within the SFB 176 (TP B11) and a travel grant to O.P., and by a grant from the University of Würzburg to C.S.B.

[2] Present address: Institute of Cell and Molecular Biology, The University of Edinburgh, Mayfield Road, Edinburgh EH9 3JH, UK.

[3] Present address: Anthropological Research Centre of the Romanian Academy, Str. Eroilor no. 8, 762421 Bucharest 4, Romania.

* Corresponding author; e-mail gerald@botanik.uni-wuerzburg.de; fax 49–931–888–6158.

Abbreviations: $[Ca^{2+}]_{cy}$, cytosolic Ca^{2+} activity; cADPR, cyclic ADP-Rib; CPA, cyclopiazonic acid; DBHQ, 2,5-di-tert-butylhydroquinone; ICP-AES, induction coupled plasma-atomic emission spectroscopy; $InsP_3$, inositol 1,4,5-trisphosphate; TMB_8, 3,4,5-trimethoxybenzoic acid 8-diethylaminooctyl ester.

MATERIALS AND METHODS

Plant Material and Solutions

The coccal green alga *Eremosphaera viridis* de Bary (Algal Culture Collection Göttingen LB 228–1, Germany) was cultured and prepared for experiments as described by Köhler et al. (1983). Algal cells with diameters of at least 150 μm were used for measurements. Under standard conditions the external medium contained 0.1 mM KNO_3, 0.1 mM $MgCl_2$, 0.1 mM $CaCl_2$, and 2 mM Mes adjusted to pH 5.6 by NaOH. For measurements at low external concentration of divalent cations, the medium contained 0.1 mM KNO_3, 1 mM EGTA, and 2 mM Mes adjusted to pH 7.6 by NaOH. Under these conditions the total $[Ca^{2+}]$ was about 1.3 μM as measured by ICP-AES. Gd^{3+} and La^{3+} were added as chloride salts and Sr^{2+} was added as a chloride salt or as carbonate or gluconate. For high external $[K^+]$, KNO_3 was used as well as the gluconate salt. TMB_8 (Biomol, Hamburg, Germany) was used as 5 mM stock solution in water. Verapamil (Biomol) and DBHQ (Biomol) were used as 10 mM stock solutions in EtOH. CPA (Biomol) was used as 5 mM stock solution in DMSO. The resulting final concentrations of EtOH or DMSO in the external medium were $\leq$ 0.5% (v/v). Control experiments showed that both solvents at concentrations $<$ 1% influenced neither the membrane potential nor cytosolic ion activities (see also Thaler et al., 1992; Sauer et al., 1993). The flow rate of the perfusion medium was adjusted to exchange the chamber volume in 1 min.

Measurement of $[Ca^{2+}]_{cy}$ and Membrane Potential

The fluorescent Ca^{2+}-sensitive dye fura-2-dextran (M_r = 10,000; Molecular Probes, Leiden, The Netherlands) was microinjected mechanically into the cytosol of the alga by a lab-made injection syringe as recently described (Plieth and Hansen, 1996). The concentration of the fluorescent dye in the cell was estimated by comparison of the fluorescence of the algal cell with the fluorescence of calibration capillaries (Plieth and Hansen, 1996). After microinjection the glass capillary was removed and a KCl-microelectrode filled with 1 M KCl was impaled to register the membrane potential in parallel with the Ca^{2+}-dependent fura-2-dextran fluorescence. The ratiometric $[Ca^{2+}]_{cy}$ measurement was performed according to the methods of Fenton and Crofts (1990) and $[Ca^{2+}]_{cy}$ was determined by in vitro calibration (Grynkiewicz et al., 1985). A detailed description of membrane potential measurement and parallel $[Ca^{2+}]_{cy}$ measurement including ratio imaging and in vitro calibration is given by Plieth and Hansen (1996). When recorded in parallel to ratiometric $[Ca^{2+}]_{cy}$ measurements, computer-aided membrane potential measurements, discontinuously synchronized to $[Ca^{2+}]_{cy}$ measurements (Plieth and Hansen, 1996), were performed. Membrane potential measurements (Axoclamp-2B, Axon Instruments, Foster City, CA) without parallel $[Ca^{2+}]_{cy}$ measurements were continuously monitored on an oscilloscope, registered by an x/t-recorder, and scanned for final analysis and presentation.

Pressure Injection of Sr^{2+}, Ca^{2+}, Ruthenium Red, and Ryanodine

To increase directly the cytosolic Sr^{2+} activity, Sr^{2+} was microinjected into a single algal cell (Förster, 1990). A glass capillary containing 0.5 mM or 1 mM $SrCl_2$ was connected via a polyethylene tube to a compressed-air cylinder and was impaled into the alga. For microinjection the turgor of the algal cell was decreased by 200 mM sorbitol in the external perfusion medium and a pressure of about 0.5 to 1.0 MPa was applied to the capillary, resulting in injection rates of 10 to 50 pL min^{-1}. Internal concentrations were estimated from the volume of the cytoplasm and the rates of microinjection. The diameter of the spherical algae ($\geq$ 150 μm) was measured for each experiment and the volume of the cytoplasm was calculated from the whole cell volume assuming 20% cytoplasm (Bethmann et al., 1995). The Sr^{2+} influx rates during microinjection ranged from 5 fmol min^{-1} (0.5 mM at 10 pL min^{-1}) to 50 fmol min^{-1} (1 mM at 50 pL min^{-1}). At 1 mM external $SrCl_2$ an initial uptake rate of 4 μM min^{-1} corresponding to 15 fmol min^{-1} was calculated (see below) from cation uptake measurements shown in Figure 8. Ca^{2+}, ruthenium red (Sigma-Aldrich, Deisenhofen, Germany), and ryanodine (Biomol) were microinjected in the same way by glass capillaries containing 0.1 mM $CaCl_2$, 10 μM, 100 μM, or 1 mM ruthenium red, or 2 mM ryanodine in water. When Sr^{2+}, Ca^{2+}, ruthenium red, or ryanodine was microinjected, the membrane potential was measured continuously with an impaled microelectrode and was used as a Ca^{2+} indicator (Bauer et al., 1997). Since fura-2-dextran binds Sr^{2+}, which results in a shift of the excitation spectrum hardly distinguishable from Ca^{2+} binding (Kwan and Putney, 1990), monitoring of $[Ca^{2+}]_{cy}$ via fura-2-dextran fluorescence was not applicable for Sr^{2+} microinjection experiments.

Measurement of Cellular Cation Concentrations

The cation content of total cells (cell sap plus cell wall) and of cell sap of *E. viridis* was determined by ICP-AES analysis as described by Bethmann et al. (1995). One-milliliter probes of a dense algal suspension were taken and incubated in 500 mL of standard medium without any addition or containing 1 mM $SrCl_2$, 100 or 250 μM $GdCl_3$, 100 μM $LaCl_3$, 1 mM $SrCl_2$ plus 10 μM DBHQ, or 1 mM $SrCl_2$ plus 10 μM CPA. Samples of total cells were dried overnight at 80°C and analyzed. Samples for cell sap were heated to 100°C for 30 min and centrifuged at 4750*g* for 30 min to remove cell walls. The supernatant representing the cell sap was analyzed.

Data Analysis and Mathematical Modeling

All results in the text are given as mean $\pm$ SD. The nonlinear regression analysis of the data in Figure 8 was done with Grafit (Erithacus Software, London, UK) based on the Marquardt algorithm. A stability analysis of Equation 2 was performed by calculating the eigenvalues (Stucki and Somogyi, 1994) for different parameter sets (Mathcad, MathSoft, Cambridge, MA). For some parameter

sets yielding stable oscillations (positive eigenvalues) Equation 2 was solved numerically (Mathematica, Wolfram Research, Champaign, IL).

RESULTS

$[Ca^{2+}]_{cy}$ and membrane potential of *E. viridis* were measured simultaneously in the same algal cell. The free-running membrane potential (E/mV) under standard conditions (in 0.1 mM KNO_3, $MgCl_2$, $CaCl_2$, and 2 mM Mes adjusted to pH 5.6 by NaOH) was -84 ± 20 mV ($n = 332$), and the steady-state $[Ca^{2+}]_{cy}$ was 163 ± 42 nM ($n = 50$) based on in vitro calibrations.

The Effect of Sr^{2+} on $[Ca^{2+}]_{cy}$ and Membrane Potential

The effect of Sr^{2+} on $[Ca^{2+}]_{cy}$ and on membrane potential in *E. viridis* is shown in Figure 1. In 95% of the experiments ($n = 27$) the addition of 1 mM Sr^{2+} to the external medium induced repetitive $[Ca^{2+}]_{cy}$ spikes that were always accompanied by parallel, repetitive, transient hyperpolarizations of the plasma membrane. The repetitive transient changes of $[Ca^{2+}]_{cy}$ and of membrane potential continued for more than 2 h under continuous perfusion of 1 mM $SrCl_2$. When Sr^{2+} was removed from the external medium the repetitive changes continued in 54% of all measurements with a decreasing frequency; 1 mM $SrCO_3$ or 1 mM Sr^{2+} gluconate had the same effect as 1 mM $SrCl_2$. In the presence of Sr^{2+} a systrophe (a chloroplast translocation to the center of the cell) was frequently observed.

The discrete $[Ca^{2+}]_{cy}$ spikes in *E. viridis* had a duration of 24 ± 8 s ($n = 28$) with a rapid rising phase and a rapid falling phase, and were separated by intervals with a constant baseline of $[Ca^{2+}]_{cy}$. The $[Ca^{2+}]_{cy}$ spikes had an amplitude of about 365 ± 71 nM ($n = 36$). Amplitudes of up to 900 nM were observed (see Fig. 4). The baseline value of $[Ca^{2+}]_{cy}$ during Sr^{2+}-induced oscillations was 168 ± 43 nM ($n = 27$). This did not differ significantly from the steady-state value of 163 ± 42 nM in the absence of $SrCl_2$ mentioned above. The duration of a single transient hyperpolarization of the plasma membrane was 35 ± 9 s with an amplitude of -181 ± 7 mV ($n = 68$). The frequency of Sr^{2+}-induced $[Ca^{2+}]_{cy}$ oscillations ranged from up to 0.8 min^{-1} (see Fig. 1) to 0.2 min^{-1} (see Fig. 5) and less. A quantitative analysis showed that lower frequencies (< 0.3 min^{-1}) were correlated with cytosolic fura-2-dextran concentrations above 10 μM (2 μM referring to the whole cell).

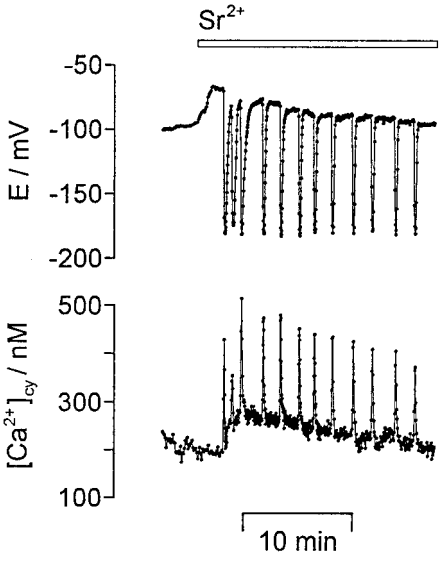

Figure 1. Sr^{2+}-induced repetitive $[Ca^{2+}]_{cy}$ spikes and repetitive transient hyperpolarizations. The $[Ca^{2+}]_{cy}$/nM (bottom) and the membrane potential (E/mV, top) were recorded simultaneously in a single algal cell. The addition of 1 mM $SrCl_2$ to the external medium (bar on top gives the perfusion protocol) induced repetitive $[Ca^{2+}]_{cy}$ spikes and parallel repetitive transient hyperpolarizations of the plasma membrane. Sampling frequency was 1/3 s^{-1}.

To investigate the dose dependency, the effect of different external $[SrCl_2]$ on the latency period and on the frequency of repetitive transient hyperpolarizations of the plasma membrane was determined (Table I). These experiments were performed as membrane potential measurements only, to avoid a frequency decrease by fura-2-dextran. The addition of 0.01 mM $SrCl_2$ had no effect on the membrane potential of *E. viridis*. The addition of increasing $[SrCl_2]$ caused increasing depolarizations (Table I, ΔE). After a latency period, τ, which decreased at larger $[SrCl_2]$, repetitive transient hyperpolarizations were induced in 69, 95, and 97% of the measurements at 0.1, 1, and 10 mM $SrCl_2$, respectively (Table I). The frequency, ν, increased, whereas the amplitude of the repetitive transient hyperpolarizations decreased at increasing $[SrCl_2]$ (Table I). A comparable decrease of amplitudes was observed at increasing external $[Mg^{2+}]$ for transient hyperpolarizations induced by darkening (Sauer et al., 1994). Routinely, we used 1 mM Sr^{2+} because this concentration was sufficient to induce long-lasting repetitive $[Ca^{2+}]_{cy}$ spikes with a high probability and frequency.

To test the effect of a direct increase in cytosolic $[Sr^{2+}]$, $SrCl_2$ was microinjected into the cytoplasm of the algal cell. The microinjection of $SrCl_2$ ($n = 15$) always resulted in hyperpolarizations (Fig. 2). At lower Sr^{2+} injection rates (Fig. 2A) repetitive transient hyperpolarizations were induced with a frequency comparable to those observed at 1 mM external $SrCl_2$ (compare Figs. 1 and 2A). At higher Sr^{2+} injection rates (Fig. 2B) a massive hyperpolarization of the plasma membrane occurred. The frequency of the transient hyperpolarizations increased to more than 1 min^{-1}, resulting in a "fusion" of the repetitive potential spikes to give rise to a fluctuating permanent hyperpolarization.

The effect of different concentrations of $CaCl_2$ or $MgCl_2$ in the external medium on repetitive transient hyperpolarizations induced by 0.1 or 1 mM external $SrCl_2$ was tested. Neither the probability to induce hyperpolarizations nor their duration or frequency were influenced by the external concentration of Ca^{2+} (or Mg^{2+}) in the range from about 1 μM Ca^{2+} (1 mM EGTA, pH 7.6; $n = 10$) up to 1 mM Ca^{2+} ($n = 8$) or 10 mM Mg^{2+} ($n = 7$).

Mn^{2+} was used to study the influx of divalent cations during Sr^{2+}-induced repetitive $[Ca^{2+}]_{cy}$ spikes (Fig. 3). Mn^{2+} is known to bind to fura-2 with about a 40-fold higher affinity than Ca^{2+}, and it quenches the fluorescence of the dye at all excitation wavelengths (Kwan and Putney,

Table I. *The effect of different external Sr^{2+} concentrations ([$SrCl_2$]/mM) on the membrane potential*

[$SrCl_2$]/mM	ΔE[a]	P[b]	τ[c]	ν[d]	Amplitude[e]	*n*
	mV	*%*	*min*	min^{-1}	*mV*	
0.01	0	0	–	–	–	4
0.1	7 ± 2	69	4.2 ± 1.5	0.2 ± 0.05	−191 ± 4	23
1	19 ± 4	95	0.5 ± 0.3	0.5 ± 0.2	−181 ± 7	273
10	38 ± 10	97	0.3 ± 0.4	0.5 ± 0.2	−167 ± 4	35

[a] The depolarization upon Sr^{2+} addition (see Figs. 1 and 6). [b] Probability to induce repetitive transient hyperpolarizations. [c] Lag phases after addition of Sr^{2+} before repetitive transient hyperpolarizations started. [d] Frequency of repetitive transient hyperpolarizations. [e] Maximum amplitude of the hyperpolarizations.

1990). The addition of 0.1 mM $MnCl_2$ to the external medium resulted in a continuous decrease of the fluorescence intensity at both excitation wavelengths (340 and 380 nm, Fig. 3, middle). This quenching of the fluorescence indicates a continuous Mn^{2+} influx into the cytoplasm of the cell. It resulted in an apparent increase of $[Ca^{2+}]_{cy}$ (Fig. 3, bottom), whereas membrane potential was hardly influenced (Fig. 3, top).

For a further characterization of the permeability of the plasma membrane for divalent cations, the plant plasma membrane Ca^{2+} channel blockers Gd^{3+} and La^{3+} (Huang et al., 1994; Marshall et al., 1994; Rengel, 1994; Piñeros and Tester, 1995) were used. Figure 4 shows that 1 mM $GdCl_3$ in the external medium reversibly blocked repetitive $[Ca^{2+}]_{cy}$ spikes in parallel to repetitive transient hyperpolarizations of the plasma membrane. This was observed in all measurements in which 1 mM $GdCl_3$ or $LaCl_3$ was used ($n = 7$). Investigating the concentration dependence revealed the following behavior. The addition of 100 μM $GdCl_3$ or $LaCl_3$ to the external medium had no effect on repetitive changes of $[Ca^{2+}]_{cy}$ and membrane potential induced by 1 mM $SrCl_2$ ($n = 14$). At concentrations of $GdCl_3$ or $LaCl_3$ of 200 μM, repetitive transient hyperpolarizations of the plasma membrane were influenced in all measurements. In 2 out of 10 measurements the hyperpolarizations were reversibly blocked, in 8 measurements the frequency was reduced by up to 70% as compared with the frequency in the absence of $GdCl_3$ or $LaCl_3$. Repetitive transient hyperpolarizations induced by 0.1 mM $SrCl_2$ were already reversibly blocked at 100 μM $GdCl_3$ or $LaCl_3$ ($n = 5$). This indicates that Sr^{2+} and La^{3+} or Gd^{3+} competitively interacted with the same plasma membrane Ca^{2+} channel. The transient hyperpolarization observed after a "light-off" stimulus was not affected by 100 μM $LaCl_3$ ($n = 12$) or $GdCl_3$ ($n = 10$). This shows that these trivalent cations do not block the plasma membrane K^+ channel, which gives rise to the transient hyperpolarization.

Besides La^{3+} and Gd^{3+}, the effect of the Ca^{2+} channel blocker verapamil was investigated. Verapamil (50 μM) reversibly inhibited repetitive transient hyperpolarizations induced by 1 mM $SrCl_2$ in 50% of the measurements ($n = 8$).

To test the relationship between the transient hyperpolarization of the plasma membrane and the $[Ca^{2+}]_{cy}$ spike, the external $[K^+]$ ($[K^+]_{ex}$/mM) was changed during Sr^{2+}-induced repetitive $[Ca^{2+}]_{cy}$ spikes. As shown in Figure 5A, an increase of $[K^+]_{ex}$ from 0.1 to 1 to 10 and finally to 100 mM decreased the amplitude of the transient hyperpolarizations. In contrast to this, the amplitude of the $[Ca^{2+}]_{cy}$ spikes (321 ± 19 nM, $n = 17$) was not influenced by $[K^+]_{ex}$ even at 100 mM. Figure 5B shows that a 10-fold increase in $[K^+]_{ex}$ resulted in a decrease of the amplitude of transient hyperpolarizations of about 54 mV, following the Nernst potential for K^+. The steady-state membrane potential became less negative at $[K^+]_{ex} > 1$ mM ($n = 8$). Depending on

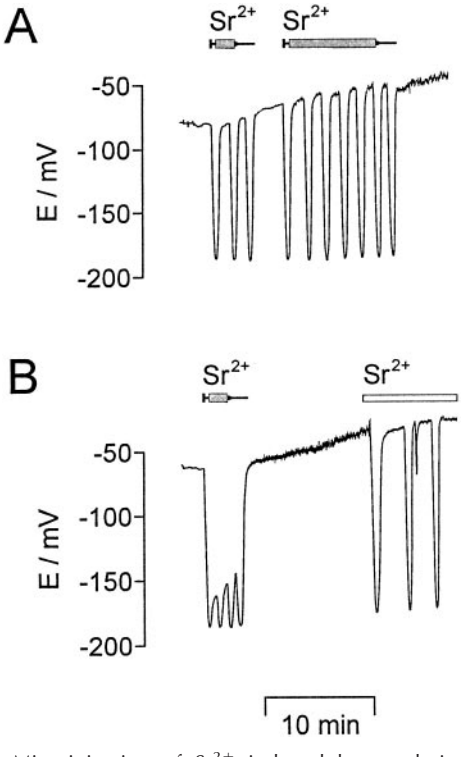

Figure 2. Microinjection of Sr^{2+} induced hyperpolarizations. A, With 0.5 mM $SrCl_2$ inside the injection pipette and small injection rates (about 10 pL/min) repetitive transient hyperpolarizations were induced as long as pressure was applied (small syringes on top indicate the duration of pressure application). B, $SrCl_2$ (1 mM) inside the injection pipette and larger injection rates (about 50 pL/min) resulted in a nearly permanent hyperpolarization as long as pressure was applied (duration indicated by the small syringe above). When a Sr^{2+} injection was followed by the external perfusion of 1 mM $SrCl_2$ (duration indicated by white bar), repetitive transient hyperpolarizations were observed. During long-lasting microinjection experiments, a continuous depolarization of the plasma membrane was frequently observed. The membrane potential was registered continuously.

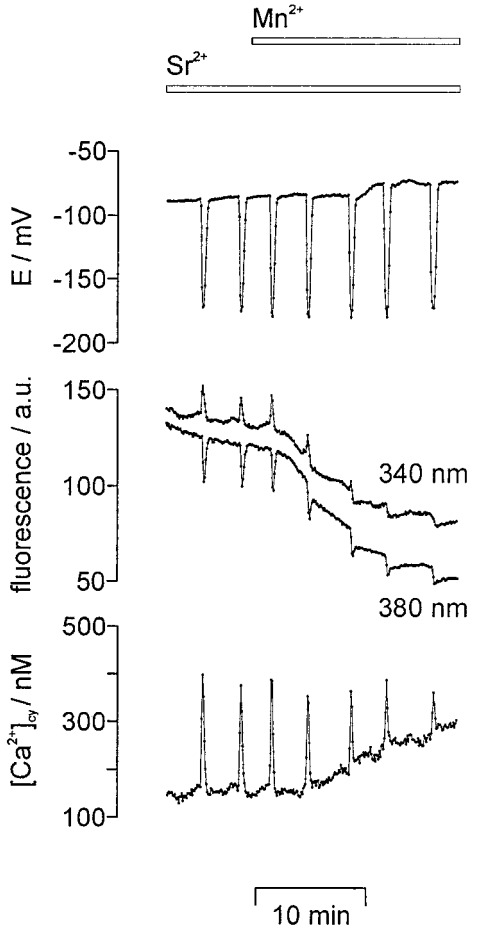

Figure 3. Mn^{2+} quenched the fura-2-dextran fluorescence intensity. Repetitive $[Ca^{2+}]_{cy}$ spikes (bottom) and repetitive transient hyperpolarizations of the plasma membrane (E/mV, top) were induced by 1 mM $SrCl_2$ in the external medium. The additional perfusion of 0.1 mM $MnCl_2$ (bars on top) decreased the fluorescence intensity emitted by fura-2-dextran (middle traces, given in arbitrary units, a.u.) at both excitation wavelengths, 340 nm (shifted upward by 25 a.u. for clarity) and 380 nm. Sampling frequency was 1/6 s^{-1}.

the steady-state membrane potential, the transient potential changes in the presence of 100 mM K^+ resulted in small transient hyperpolarizations or small transient depolarizations. Even $[Ca^{2+}]_{cy}$ spikes accompanied by a transient depolarization of the plasma membrane did not significantly differ from those observed under standard conditions (0.1 mM KNO_3), as shown in Figure 5A. K^+ gluconate had the same effect as KCl.

To study the involvement of internal Ca^{2+} stores, the effect of the ER Ca^{2+}-ATPase blockers DBHQ and CPA (Inesi and Sagara, 1994) on Sr^{2+}-induced repetitive $[Ca^{2+}]_{cy}$ spikes was investigated. As shown in Figure 6, repetitive $[Ca^{2+}]_{cy}$ spikes and repetitive transient hyperpolarizations were inhibited by 10 μM DBHQ after 2.9 ± 1.2 min (n = 8). The inhibitory effect was reversible when DBHQ was washed out for more than 20 min (n = 7). After a 5-min preperfusion of 10 μM DBHQ, the addition of Sr^{2+} (n = 8) induced one or a few repetitive transient hyperpolarizations with reduced amplitudes, but never sustained oscillations (not shown). Longer preperfusions inhibited Sr^{2+}-induced transient hyperpolarizations. CPA at a concentration of 10 μM had the same effects on Sr^{2+}-induced repetitive transient hyperpolarizations as 10 μM DBHQ (n = 5). The baseline $[Ca^{2+}]_{cy}$ level was not increased in the presence of DBHQ (Fig. 6), showing that a cytosolic Ca^{2+} homeostasis was still achieved by active Ca^{2+} transport systems that are not sensitive to DBHQ. A transient hyperpolarization induced by pressure injection of Ca^{2+} was not affected by 10 μM DBHQ, indicating that DBHQ did not act on the Ca^{2+}-dependent plasma membrane K^+ channel.

TMB_8, an antagonist of $InsP_3$-induced Ca^{2+} release from intracellular stores in animal (Zhang and Melvin, 1993) and plant cells (Schumaker and Sze, 1987; Förster, 1990), did not block Sr^{2+}-induced repetitive $[Ca^{2+}]_{cy}$ spikes and transient hyperpolarizations at concentrations up to 200 μM (n = 28).

The effect of ruthenium red (Ma, 1993) and ryanodine (Smith et al., 1988), known antagonists of the ryanodine/cADPR Ca^{2+} release channel, were investigated. Both were microinjected into the cytoplasm of algal cells either before 1 mM $SrCl_2$ was added or during Sr^{2+}-induced repetitive transient hyperpolarizations. At cytosolic ruthenium red concentrations below 10 μM the amplitudes of the transient hyperpolarizations were decreased and they were completely inhibited at ruthenium red concentrations above 10

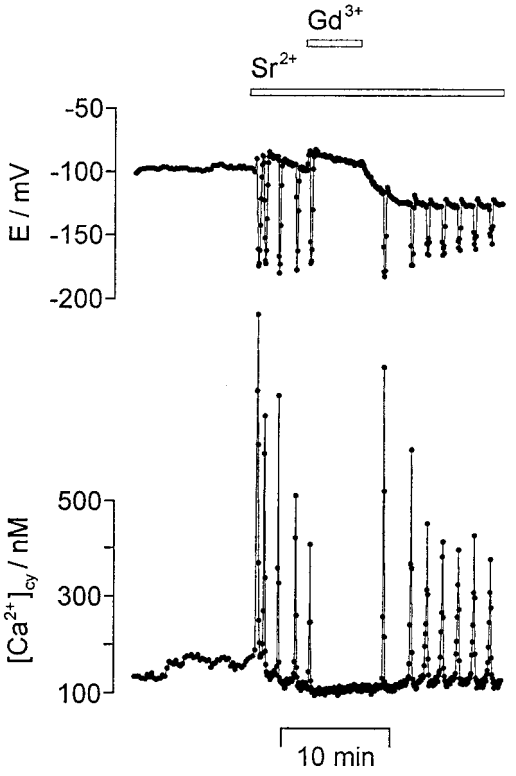

Figure 4. Gd^{3+} inhibited Sr^{2+}-induced repetitive $[Ca^{2+}]_{cy}$ spikes and repetitive transient hyperpolarizations. Repetitive $[Ca^{2+}]_{cy}$ spikes (bottom) and repetitive transient hyperpolarizations (E/mV, top) were induced by 1 mM $SrCl_2$. The additional perfusion of 1 mM $GdCl_3$ for 5 min (bars on top) reversibly inhibited the repetitive $[Ca^{2+}]_{cy}$ and potential changes. Sampling frequency was 1/1.5 s^{-1}.

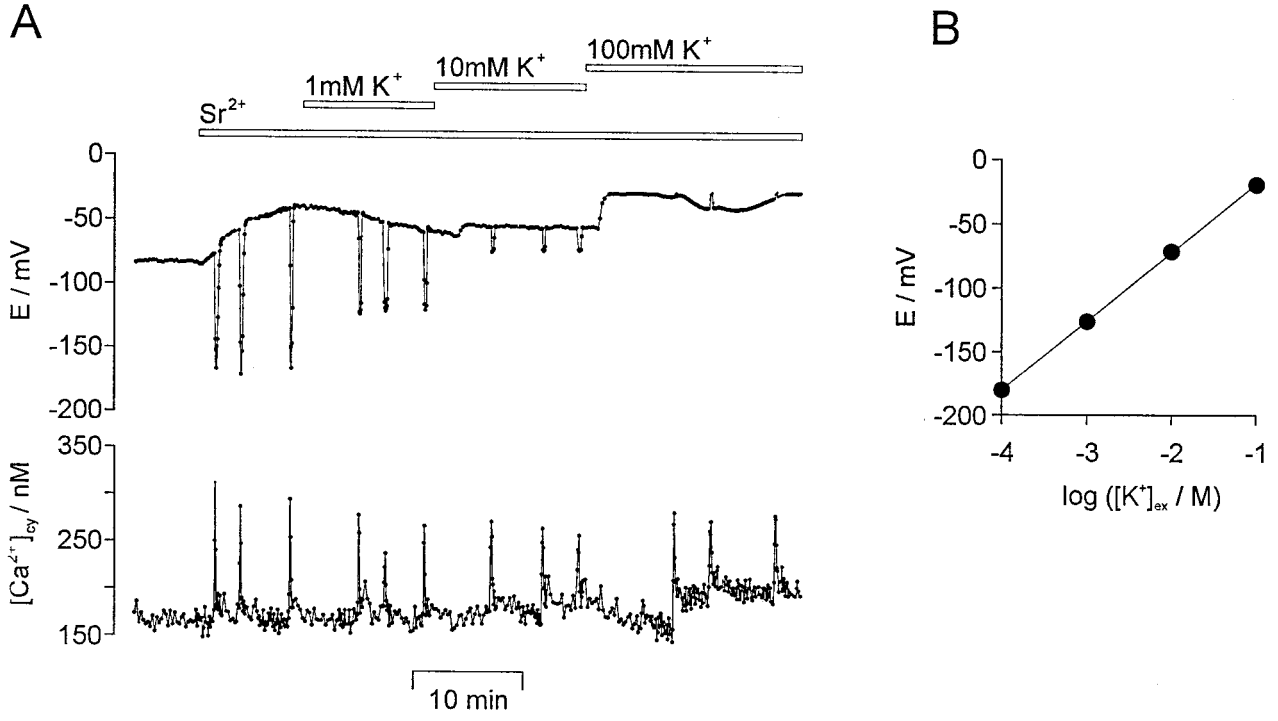

Figure 5. The effect of different external $[K^+]$ on Sr^{2+}-induced repetitive $[Ca^{2+}]_{cy}$ spikes and repetitive transient hyperpolarizations. A, Repetitive $[Ca^{2+}]_{cy}$ spikes (bottom) and repetitive transient hyperpolarizations (E/mV, top) were induced by the addition of 1 mM $SrCl_2$ to the medium. The external $[K^+]$ was increased from 0.1 mM KCl (standard medium) to 1 mM, to 10 mM, and finally to 100 mM (bars on top). Sampling frequency was 1/3 s^{-1}. B, The amplitude of the transient hyperpolarizations (E/mV) was plotted against the logarithm of the external $[K^+]$: log ($[K^+]_{ex}$/M). A linear regression analysis (solid line, r = 0.999) yielded a slope of 53.8 ± 0.4 mV for each 10-fold increase in $[K^+]$. Data points are given as means ± SE (n = 15) with SE being smaller than the symbol size.

μM (n = 21) (Fig. 7). At cytosolic ryanodine concentrations below 100 μM, amplitudes and frequency of transient hyperpolarizations were decreased. At cytosolic ryanodine concentrations above 100 μM, Sr^{2+}-induced repetitive transient hyperpolarizations were completely blocked (n = 6). The transient hyperpolarization observed after a "light-off" stimulus was influenced neither by ruthenium red (Fig. 7) nor by ryanodine at concentrations as high as several hundred micrometers.

Measurements of Cation Uptake

To investigate whether Sr^{2+} enters *E. viridis*, algal cells were incubated in the standard medium containing additionally 1 mM $SrCl_2$, and the $[Sr^{2+}]$ ($[Sr^{2+}]/\mu$M) of the total cells (cell sap plus cell wall) and the cell sap were determined after different incubation times. As shown in Figure 8, the $[Sr^{2+}]$ of the cell sap increased, reaching a stable value within 2 to 3 h. In the presence of 10 μM DBHQ or CPA, Sr^{2+} uptake into *E. viridis* was not significantly influenced (Fig. 8). The average (n = 14) $[Sr^{2+}]$ of the total cells was 24 μM larger compared with the concentration in the cell sap, regardless of the incubation time. This reflects a constant amount of Sr^{2+}, which was bound to the cell wall. The time course of the increase of the $[Sr^{2+}]$ in the cell sap was mathematically described under the assumption that the Sr^{2+} influx was compensated by a Sr^{2+} export that

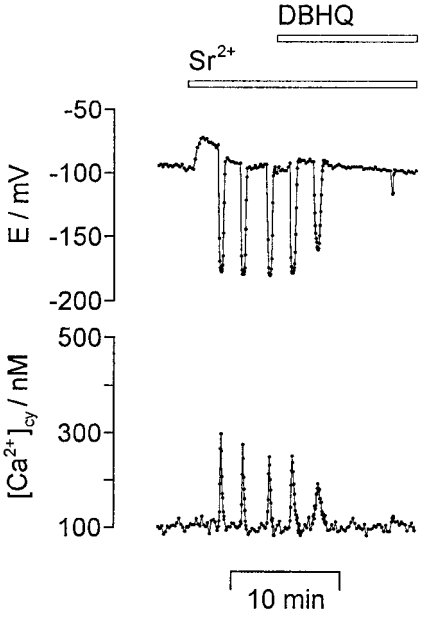

Figure 6. The ER Ca^{2+}-ATPase inhibitor DBHQ blocked Sr^{2+}-induced repetitive $[Ca^{2+}]_{cy}$ spikes and repetitive transient hyperpolarizations. Repetitive $[Ca^{2+}]_{cy}$ spikes (bottom) and repetitive transient hyperpolarizations (E/mV, top) induced by 1 mM $SrCl_2$ were inhibited after the addition of 10 μM DBHQ to the external medium (bars on top). Sampling frequency was 1/3 s^{-1}.

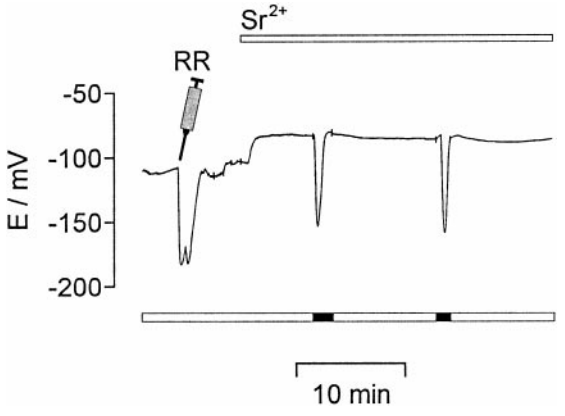

Figure 7. The ryanodine/cADPR Ca^{2+} release channel antagonist ruthenium red (RR) blocked Sr^{2+}-induced hyperpolarizations. With 1 mM inside the pipette ruthenium red was microinjected (indicated by the syringe), resulting in a cytosolic concentration of about 100 μM. The microinjection itself caused a transient hyperpolarization. Afterward the addition of 1 mM $SrCl_2$ to the external medium failed to induce any hyperpolarization, whereas darkening (light protocol given by the bars below) still induced a transient hyperpolarization. The membrane potential was recorded continuously.

linearly increases with internal $[Sr^{2+}]$: $[Sr^{2+}]$ starts at an initial value $[Sr^{2+}]_0$ at $t = 0$ and reaches an equilibrium concentration $[Sr^{2+}]_{EQ}$ at $t \rightarrow \infty$ according to

$$[Sr^{2+}] = [Sr^{2+}]_{EQ} + ([Sr^{2+}]_0 - [Sr^{2+}]_{EQ}) \cdot \exp(-a \cdot t) \quad (1)$$

where a is the rate constant in min^{-1}. The initial $[Sr^{2+}]$ of the cell sap was determined by ICP-AES analysis before Sr^{2+} was added to the external medium as $[Sr^{2+}]_0 = 2.1 \pm 0.75$ μM ($n = 5$). On the basis of Equation 1, a nonlinear regression analysis of the data points summarized in Figure 8 yielded an equilibrium $[Sr^{2+}]$ of the cell sap of $[Sr^{2+}]_{EQ} = 200$ μM and a rate constant of $a = 0.02$ min^{-1}. From these data, using the first derivation of Equation 1, an initial Sr^{2+} influx at $t = 0$ of 4.0 μM min^{-1} was calculated that corresponds to a current of about 24 pA for a spherical algal cell with a diameter of 150 μm (34 $\mu A\ cm^{-2}$).

Besides Sr^{2+}, the concentrations of La^{3+} and Gd^{3+} were measured in the total cells and in the cell sap of *E. viridis* after 60 min of incubation at 100 μM $LaCl_3$ or up to 250 μM $GdCl_3$ in the external medium, respectively. The $[La^{3+}]$ in the total cells was about 1.0 mM, whereas the $[La^{3+}]$ in the cell sap was below the detection limit of about 0.8 μM. Similar values were obtained for Gd^{3+}. A concentration of about 0.5 mM Gd^{3+} was measured for total cells whereas the concentration in the cell sap remained below the detection limit of about 1.0 μM. This indicates that La^{3+} and Gd^{3+} were not taken up into *E. viridis* to a considerable amount. It also demonstrated that a proper separation of the cell wall from the cell sap was achieved. In the presence of 250 μM $GdCl_3$, Sr^{2+} uptake after 60 min was decreased from about 145 to 59 μM.

DISCUSSION

There are two fundamental questions about $[Ca^{2+}]_{cy}$ oscillations: How do they arise? And what is their physiological function? The above measurements provide access to the understanding of the mechanism of $[Ca^{2+}]_{cy}$ oscillations in a green plant cell. In this context Sr^{2+} was used as a tool to induce long-lasting repetitive $[Ca^{2+}]_{cy}$ spikes. In animal cells Sr^{2+} is frequently used to induce Ca^{2+} release from intracellular Ca^{2+} stores (Mironov and Juri, 1990; Grégoire et al., 1993) and Sr^{2+} was shown to induce repetitive Ca^{2+} spikes (Bos-Mikich et al., 1995). Regarding the physiological response to increasing $[Ca^{2+}]_{cy}$ in *E. viridis*, it should be mentioned that $[Ca^{2+}]_{cy}$ oscillations are accompanied by a systrophe, which is a chloroplast translocation to the center of the cell (Schönknecht et al., 1998). This systrophe is observed as a reaction to excess light and is also induced in *E. viridis* by blue light in the presence of external Ca^{2+} (Weidinger and Ruppel, 1985).

Sr^{2+} Uptake and Compartmentalization

Sr^{2+} was rapidly taken up into *E. viridis*, as shown in Figure 8. It is known that binding of Sr^{2+} to fura-2-dextran results in a fluorescence excitation spectrum very similar to the spectrum caused by Ca^{2+}, with a 30-fold lower affinity of fura-2-dextran for Sr^{2+} compared with Ca^{2+} (Kwan and

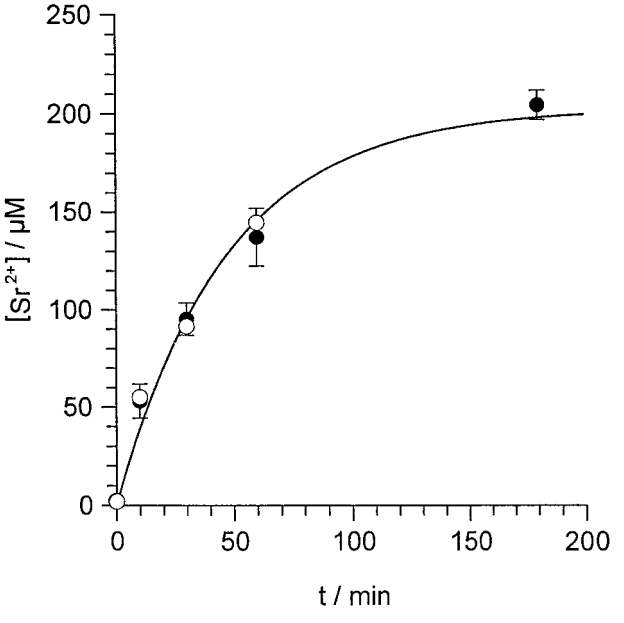

Figure 8. Sr^{2+} uptake into *E. viridis*. Algal cells were incubated in the standard medium plus 1 mM $SrCl_2$ either containing no ER Ca^{2+}-ATPase inhibitor (control, ●) or containing additionally 10 μM DBHQ or CPA (○). After different incubation times (t/min) cells were separated from the medium and the $[Sr^{2+}]$ of the cell sap ($[Sr^{2+}]/\mu M$) was determined. Data points of the control (●) are given as means ± SE of three to six measurements; data points measured in the presence of ER Ca^{2+}-ATPase inhibitors (○) are means of three measurements. Data points were described by Equation 1. With an initial $[Sr^{2+}]$ of $[Sr^{2+}]_0 = 2.1$ μM, a fit to 19 separate data points for the control (●) yielded an equilibrium $[Sr^{2+}]$ of $[Sr^{2+}]_{EQ} = 204 \pm 18$ μM, and a rate constant of $a = 0.021 \pm 0.004$ min^{-1} (fit indicated by the solid line). When the data points measured in the presence of ER Ca^{2+}-ATPase inhibitors (○) were included in the fit, parameters did not significantly change ($[Sr^{2+}]_{EQ} = 202 \pm 18$ μM, $a = 0.022 \pm 0.004$ min^{-1}).

Putney, 1990). The baseline value of $[Ca^{2+}]_{cy}$ during Sr^{2+}-induced oscillations did not differ from the steady-state $[Ca^{2+}]_{cy}$ level in the absence of Sr^{2+} (see Figs. 1, 4, 5A, and 6). Therefore, the free cytosolic Sr^{2+} activity did not exceed 1 to 2 μM. On the other hand, $[Sr^{2+}]$ of up to 200 μM were measured in the cell sap. This shows that Sr^{2+} was effectively compartmentalized into internal organelles, which is comparable to animal cells (Kwan and Putney, 1990; Mironov and Juri, 1990). As documented in Figure 2, besides being effective, the intracellular compartmentalization of Sr^{2+} was also rapid; immediately after stopping Sr^{2+} microinjection membrane potential oscillations ceased. The only organelle that can contribute to the measured intracellular steady-state concentration of 200 μM Sr^{2+} (Fig. 8) is the vacuole. All other organelles have such a small volume compared with the total volume of the cell (1.8 nL), that an accumulation of this amount of Sr^{2+} (360 fmol) in another compartment is unlikely. A vacuolar $[Sr^{2+}]$ of 250 μM (80% of the cell volume) is comparable to the vacuolar $[Ca^{2+}]$ of about 400 μM in *E. viridis* (Bethmann et al., 1995). The plasma membrane Ca^{2+} channel blocker Gd^{3+} (Marshall et al., 1994; Rengel, 1994; Piñeros and Tester, 1995) considerably decreased Sr^{2+} uptake. Sr^{2+} uptake and compartmentalization were not affected by the ER Ca^{2+}-ATPase blockers CPA or DBHQ (Fig. 8), indicating that these inhibitors influenced neither the Sr^{2+} influx and efflux across the plasma membrane (compare Eq. 1) nor Sr^{2+} uptake into the vacuole (summarized in Fig. 10).

Sr^{2+}-Induced Repetitive $[Ca^{2+}]_{cy}$ Spikes in *E. viridis* Show a Baseline Spiking Pattern

$[Ca^{2+}]_{cy}$ oscillations in animal and plant cells display a variety of patterns. Besides more irregular repetitive $[Ca^{2+}]_{cy}$ changes, sinusoidal $[Ca^{2+}]_{cy}$ oscillations are observed, which differ from baseline spiking $[Ca^{2+}]_{cy}$ oscillations displaying discrete $[Ca^{2+}]_{cy}$ spikes separated by a baseline of $[Ca^{2+}]_{cy}$ (Fewtrell, 1993). In animal cells sinusoidal $[Ca^{2+}]_{cy}$ oscillations and baseline spiking $[Ca^{2+}]_{cy}$ oscillations are mechanistically different. Whereas for sinusoidal $[Ca^{2+}]_{cy}$ oscillations the agonist dose increases the amplitude but not the frequency, for baseline spiking $[Ca^{2+}]_{cy}$ oscillations the frequency is determined by the agonist dose, whereas the amplitude is independent from the agonist dose, and the latency period before the first $[Ca^{2+}]_{cy}$ spike is inversely related to the agonist dose (Thomas et al., 1996). Furthermore, Ca^{2+} signals with a baseline spiking pattern continue for a long period of stimulation. The agonist dose dependency of Sr^{2+}-induced baseline spiking oscillations in *E. viridis* is the same. The frequency increased with increasing external $[Sr^{2+}]$ (Table I), as well as with increasing microinjected $[Sr^{2+}]$ (Fig. 2). The latency period decreased with increasing external $[Sr^{2+}]$ (Table I). Moreover, Sr^{2+}-induced repetitive $[Ca^{2+}]_{cy}$ spikes in *E. viridis* lasted a very long time. Not only the pattern but also the dose dependency of the repetitive $[Ca^{2+}]_{cy}$ spikes observed in *E. viridis* was comparable to animal cells. This is the first indication to our knowledge that similar patterns of $[Ca^{2+}]_{cy}$ oscillations in plant and animal cells may be based on a similar mechanism.

Changes in $[Ca^{2+}]_{cy}$ are involved in many different signal transduction processes (Trewavas et al., 1996; Webb et al., 1996), which raises the question of how a stimulus specificity is achieved. $[Ca^{2+}]_{cy}$ oscillations may encode information about the stimulus by the frequency, amplitude, or duration (Clapham, 1995; Berridge, 1997). In animal cells there is considerable evidence that frequency encoding does contribute to a stimulus-specific reaction: $[Ca^{2+}]_{cy}$ oscillations have been shown to depend on the type or strength of a stimulus (Petersen et al., 1994; Thomas et al., 1996), and biochemical mechanisms are documented that are able to decode $[Ca^{2+}]_{cy}$ oscillations (Hajnóczky et al., 1995; De Koninck and Schulman, 1998). Agonist-induced frequency modulation has not been shown in plants, but the results presented here suggest that the relevant mechanisms for frequency encoding exist in *E. viridis*.

In *Commelina communis* guard cells an increase to 100 μM of the external $[Ca^{2+}]$ induces baseline spiking $[Ca^{2+}]_{cy}$ oscillations, however, a further increase to 1 mM results in asymmetric and irregular Ca^{2+}-induced $[Ca^{2+}]_{cy}$ elevations (McAinsh et al., 1995). In *E. viridis* the external concentration of Ca^{2+} or Mg^{2+} had no effect on Sr^{2+}-induced oscillations.

Membrane Potential Oscillations Are Caused by $[Ca^{2+}]_{cy}$ Oscillations

The measurements presented here (Figs. 1 and 3–6) demonstrate the close correlation between $[Ca^{2+}]_{cy}$ spikes and transient hyperpolarizations. This correlation raises the question of whether the $[Ca^{2+}]_{cy}$ spikes cause transient hyperpolarizations or whether the transient hyperpolarizations cause Ca^{2+} spikes. For animal cells both possibilities are well documented. On the one hand, autonomous $[Ca^{2+}]_{cy}$ oscillations driven by Ca^{2+} release from internal stores may cause membrane potential oscillations due to the opening of Ca^{2+}-dependent plasma membrane ion channels (Lee and Earm, 1994; Wojnowski et al., 1994; D'Andrea and Thorn, 1996). On the other hand, autonomous plasma membrane oscillations may cause $[Ca^{2+}]_{cy}$ oscillations due to Ca^{2+} influx via voltage-dependent Ca^{2+} channels (Li et al., 1995b; Larsson et al., 1996). Within the time resolution of our measurements (1.5–6 s) $[Ca^{2+}]_{cy}$ normally increased at the same time as the membrane potential started to hyperpolarize. The experiments illustrated in Figure 5 show that the plasma membrane potential as changed by external $[K^+]$ does not exert any significant effect on Sr^{2+}-induced $[Ca^{2+}]_{cy}$ spikes. This is opposite to what is expected for $[Ca^{2+}]_{cy}$ spikes caused by an influx of Ca^{2+} across the plasma membrane. Such $[Ca^{2+}]_{cy}$ spikes vary with the membrane potential, but this was not observed (Fig. 5). Even when the transient hyperpolarization switched to a depolarization, the amplitude and time course of the $[Ca^{2+}]_{cy}$ spikes were not influenced. This clearly shows that the $[Ca^{2+}]_{cy}$ spikes caused the membrane potential changes rather than the other way around. The close correlation between $[Ca^{2+}]_{cy}$ spikes and transient hyperpolarizations in *E. viridis* (Figs. 1 and 3–6;

Bauer et al., 1997) is due to the Ca^{2+}-dependent opening of plasma membrane K^+ channels (Fig. 5B).

The Role of Ca^{2+} Release and Re-Uptake by Internal Stores

Most models describing the mechanism of $[Ca^{2+}]_{cy}$ oscillations in animal cells are based on a repetitive Ca^{2+} release and re-uptake by intracellular Ca^{2+} stores (Tsien and Tsien, 1990; Fewtrell, 1993; Petersen et al., 1994). We used DBHQ (Fig. 6) and CPA to demonstrate the role of Ca^{2+} release and re-uptake by intracellular Ca^{2+} stores for $[Ca^{2+}]_{cy}$ oscillations in *E. viridis*. CPA and DBHQ are well-established inhibitors of ER Ca^{2+}-ATPases in animal cells (Inesi and Sagara, 1994). In plant cells DBHQ and CPA recently have been shown to act specifically on ER Ca^{2+}-ATPases as well (Logan and Venis, 1995; Hwang et al., 1997; Liang et al., 1997). Both inhibitors are lipophilic and readily enter the cell (Busch and Sievers, 1993; Du et al., 1994; Trebacz et al., 1996), which explains the long duration needed for a wash out with *E. viridis*. In line with a specific action on ER Ca^{2+}-ATPases, CPA or DBHQ influenced neither the transport of divalent cations across the plasma membrane and the tonoplast (Fig. 8) nor the steady-state $[Ca^{2+}]_{cy}$ (Fig. 6). Blocking ER Ca^{2+}-ATPases by CPA or DBHQ prevents the re-uptake of Ca^{2+} into the ER, resulting in a rapid emptying of the Ca^{2+} store that drives $[Ca^{2+}]_{cy}$ oscillations. Thus, a Sr^{2+}-induced Ca^{2+} release is no longer possible, i.e. $[Ca^{2+}]_{cy}$ oscillations come to an end.

The Role of Ca^{2+} Fluxes across the Plasma Membrane

Since plasma membrane Ca^{2+}-ATPases transport Ca^{2+} out of the cell, especially during $[Ca^{2+}]_{cy}$ spikes, a certain Ca^{2+} influx is necessary to prevent a depletion in Ca^{2+}. In animal cells Ca^{2+} fluxes across the plasma membrane have been shown to be substantial for sustained $[Ca^{2+}]_{cy}$ oscillations (Tsien and Tsien, 1990; Fewtrell, 1993; Petersen et al., 1994). The quenching of the fura-2-dextran fluorescence by externally added Mn^{2+} (Kwan and Putney, 1990) (Fig. 3) indicated that the plasma membrane of *E. viridis* had a significant permeability for Mn^{2+}, which is known to permeate plant plasma membrane Ca^{2+} channels (Piñeros and Tester, 1995).

During transient hyperpolarizations Mn^{2+} quenching significantly increased (Fig. 3). This could be caused by the increasing electrical driving force for Mn^{2+} influx and does not necessarily point to a voltage-dependent conductance increase. An increasing Mn^{2+} quenching indicates an increasing Ca^{2+} influx, suggesting that a component of the $[Ca^{2+}]_{cy}$ spikes might arise directly via Ca^{2+} influx during the transient hyperpolarization. However, neither the external $[Ca^{2+}]$ nor the membrane potential (see Fig. 5) have a significant influence on $[Ca^{2+}]_{cy}$ spike amplitudes. Therefore, a Ca^{2+} influx during transient hyperpolarizations does not seem to contribute significantly to $[Ca^{2+}]_{cy}$ spike amplitudes.

The application of the plant plasma membrane Ca^{2+} channel blockers La^{3+} or Gd^{3+} (Huang et al., 1994; Marshall et al., 1994; Rengel, 1994; Piñeros and Tester, 1995) reversibly inhibited Sr^{2+}-induced repetitive $[Ca^{2+}]_{cy}$ spikes and transient hyperpolarizations in *E. viridis* (Fig. 4). The cation uptake measurements showed that neither La^{3+} nor Gd^{3+} reached micromolar intracellular concentrations, which were reported to block ER (Klüsener et al., 1995) or tonoplast Ca^{2+} channels (Johannes et al., 1992; Pantoja et al., 1992). Therefore, La^{3+} and Gd^{3+} are very likely to act on plasma membrane Ca^{2+} channels. Accordingly, the dark-induced transient hyperpolarization that is caused by a single $[Ca^{2+}]_{cy}$ spike in *E. viridis* (Bauer et al., 1997), probably due to Ca^{2+} release from the chloroplast (Schönknecht et al., 1998), was not affected by these plasma membrane Ca^{2+} channel blockers. As the results in Figure 5 show, $[Ca^{2+}]_{cy}$ spikes in *E. viridis* are not caused by membrane potential-driven Ca^{2+} influx. However, the inhibitory effect of La^{3+} or Gd^{3+} indicates that, comparable to animal cells, a certain Ca^{2+} influx across the plasma membrane is necessary for sustained $[Ca^{2+}]_{cy}$ oscillations. Since La^{3+} or Gd^{3+} also block Sr^{2+} uptake, and Sr^{2+} is rapidly compartmentalized at the same time, the effect of the trivalent cations may alternatively be explained by a decrease of the cytosolic Sr^{2+} activity, resulting in cessation of oscillations. However, caffeine-induced repetitive $[Ca^{2+}]_{cy}$ spikes in *E. viridis* have recently been shown to be reversibly inhibited by La^{3+} or Gd^{3+} as well (Bauer et al., 1997), corroborating the view that a certain Ca^{2+} influx is essential for sustained $[Ca^{2+}]_{cy}$ oscillations.

A Mathematical Model for Sr^{2+}-Induced Repetitive $[Ca^{2+}]_{cy}$ Spikes

On the basis of the results mentioned above, it becomes possible to describe the repetitive $[Ca^{2+}]_{cy}$ spikes in *E. viridis* theoretically by adapting a mathematical model proposed by Stucki and Somoggyi (1994).

$$\begin{cases} \dfrac{dy}{dt} = A - (b + c)\cdot y + \left(\alpha + \beta\cdot\dfrac{(y + Sr)^n}{K^n + (y + Sr)^n}\right)\cdot(x - y) \\ \dfrac{dx}{dt} = c\cdot y - \left(\alpha + \beta\cdot\dfrac{(y + Sr)^n}{K^n + (y + Sr)^n}\right)\cdot(x - y) \end{cases} \tag{2}$$

The two differential equations describe the changes of the Ca^{2+} activities in the cytosol and in the store due to the repetitive release and re-uptake of Ca^{2+} by internal stores plus Ca^{2+} fluxes across the plasma membrane. This is illustrated in Figure 9A. $y = [Ca^{2+}]_{cy}$ is increased by a steady influx A across the plasma membrane. Ca^{2+}-ATPases pump cytosolic Ca^{2+} into internal stores (c) or across the plasma membrane (b) with a rate proportional to y. The fluxes out of the store depend on the difference between the Ca^{2+} activities in the store and in the cytosol (x–y). There is a linear leak (α), and a Ca^{2+} release channel (β), which is assumed to be modulated in a cooperative manner (K, n) by cytosolic Ca^{2+} (y) and Sr^{2+} (Sr in Eq. 2) activities. The change in Ca^{2+} activity inside the store x is determined by the balance of the flux into the store ($c \cdot y$) and the fluxes out of the store already mentioned. The assumption of a Sr^{2+}-induced Ca^{2+} release is a feature additionally introduced to the original mathematical

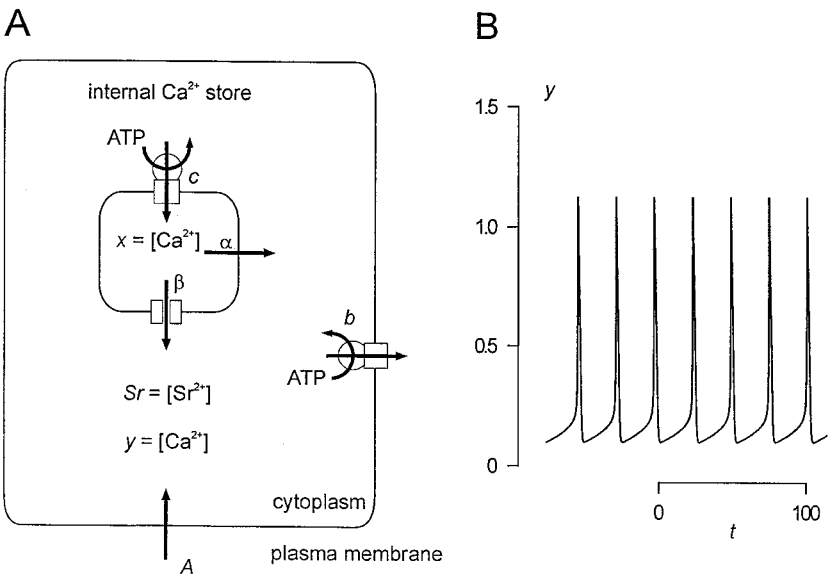

Figure 9. A theoretical model of the repetitive $[Ca^{2+}]_{cy}$ spikes in *E. viridis*. A, Schematic model of the Ca^{2+} fluxes involved in generating repetitive $[Ca^{2+}]_{cy}$ spikes in *E. viridis*. The $[Ca^{2+}]_{cy}$, *y*, and Sr^{2+} activity, *Sr*, cause a Ca^{2+}/Sr^{2+}-induced Ca^{2+} release (β) from an internal Ca^{2+} store. The Ca^{2+} store is refilled by a Ca^{2+}-ATPase (*c*), and there is a continuous Ca^{2+} efflux due to a "leak" (α). A plasma membrane Ca^{2+}-ATPase removes Ca^{2+} from the cytoplasm (*b*), and there is a Ca^{2+} influx from the external medium (*A*). B, Temporal response of the system depicted in A and described by Equation 2. The $[Ca^{2+}]_{cy}$, *y*, is plotted as a function of time, *t*, for: $A = 0.2$; $b = 1$; $c = 2$; $\alpha = 0.05$; $\beta = 15.7$; $K = 1$; $Sr = 0.1$; $n = 4$; $x(t=0) = 2.8$; $y(t=0) = 0.2$. For the sake of simplicity no units are given and the axes are given in arbitrary units.

model of Stucki and Somogyi (1994). This Sr^{2+} dependence is established for different animal cells (Mironov and Juri, 1990; Grégoire et al., 1993). Figure 9B demonstrates that this theoretical approach is sufficient to model $[Ca^{2+}]_{cy}$ oscillations with a baseline spiking pattern. With the parameters chosen for Figure 9B there are no oscillations in the absence of Sr^{2+} ($Sr = 0$) in the cytoplasm. Only in the presence of a certain amount of Sr^{2+} is Ca^{2+} released by the Ca^{2+} release channel from the intracellular Ca^{2+} store, initiating sustained $[Ca^{2+}]_{cy}$ oscillations.

The theoretical model described by Equation 2 and depicted in Figure 9 is a minimal model that does not consider buffer capacities, the influx and compartmentalization of Sr^{2+}, or the volumes of different compartments. However, it contains all the elements discussed above (see Fig. 10): An intracellular Ca^{2+} store that is filled by a DBHQ or CPA-sensitive Ca^{2+}-ATPase, a continuous Ca^{2+} efflux from the Ca^{2+} store, which slowly depletes the store when the Ca^{2+}-ATPase is blocked, and a Ca^{2+} influx pathway across the plasma membrane that is blocked by Gd^{3+} or La^{3+}.

The Nature of the Ca^{2+} Release

Most $[Ca^{2+}]_{cy}$ oscillations investigated in nonexcitable animal cells turned out to be caused by Ca^{2+} release via the $InsP_3$-activated Ca^{2+} channel (Berridge, 1993; Fewtrell, 1993; Li et al., 1995a). TMB_8, which was shown to inhibit $InsP_3$-induced Ca^{2+} release in *E. viridis* (Förster, 1990), had no effect on Sr^{2+}-induced $[Ca^{2+}]_{cy}$ oscillations, indicating that $InsP_3$-activated Ca^{2+} channels are not involved. In animal cells, besides caffeine, Sr^{2+} is known to induce Ca^{2+} release from internal stores via the ryanodine/cADPR Ca^{2+} channel (Meissner, 1994; Lee et al., 1995). In *E. viridis* caffeine and Sr^{2+} alike induce repetitive $[Ca^{2+}]_{cy}$ spikes and transient hyperpolarizations (Bauer et al., 1997). Ruthenium red (Ma, 1993) and ryanodine (Smith et al., 1988) are known to be specific for the ryanodine/cADPR Ca^{2+} channel, not interacting with the $InsP_3$-activated Ca^{2+} channel (Ehrlich et al., 1994). Ruthenium red and ryanodine were recently shown to block Ca^{2+} release in plant cells as well (Allen et al., 1995; Muir and Sanders, 1996). Both inhibitors when microinjected into *E. viridis* blocked Sr^{2+}-induced repetitive transient hyperpolarizations (Fig. 7). Neither ruthenium red (Fig. 7) nor ryanodine affected the transient hyperpolarization observed after darkening, indicating that both inhibitors specifically blocked Sr^{2+}-induced Ca^{2+} release and not the $[Ca^{2+}]_{cy}$ spike induced by darkening (Bauer et al., 1997). Most likely, in *E. viridis* Sr^{2+} induced a Ca^{2+} release from intracellular Ca^{2+} stores by activating a type of ryanodine/cADPR Ca^{2+} channel (Fig. 10).

Probably this ryanodine/cADPR Ca^{2+} channel is located in the ER (Fig. 10). This is evident from the effect of CPA or DBHQ, which specifically inhibit ER Ca^{2+}-ATPases in animal (Inesi and Sagara, 1994) as well as in plant cells (Logan and Venis, 1995). As discussed above, in *E. viridis* CPA or DBHQ influenced neither the transport of divalent cations across the plasma membrane and the tonoplast (Fig. 8) nor the steady-state $[Ca^{2+}]_{cy}$ (Fig. 6). Moreover, a preperfusion of DBHQ or CPA for more than 5 min completely blocked Sr^{2+}-induced oscillations, indicating a rather small volume or Ca^{2+} content of the affected Ca^{2+} store. In *E. viridis* as in animal cells (Kass et al., 1989; Demaurex et al., 1992), there is probably a continuous Ca^{2+} efflux from the store and when the compensating Ca^{2+} uptake by Ca^{2+}-ATPases is blocked, this results in a Ca^{2+} store depletion even in the absence of Sr^{2+}-induced $[Ca^{2+}]_{cy}$ oscillations. This depletion within a few minutes excludes the involvement of the vacuole, since the vacuole is a huge store of free Ca^{2+} in *E. viridis* (Bethmann et al., 1995). Little is known about Ca^{2+} release channels of the plant ER. Klüsener et al. (1995) isolated and reconstituted a voltage-dependent Ca^{2+} channel from the ER of a higher plant mechanoreceptor organ that was not affected by $InsP_3$ or ryanodine. In *E. viridis* as in other plant cells, the vacuole is the largest internal Ca^{2+}

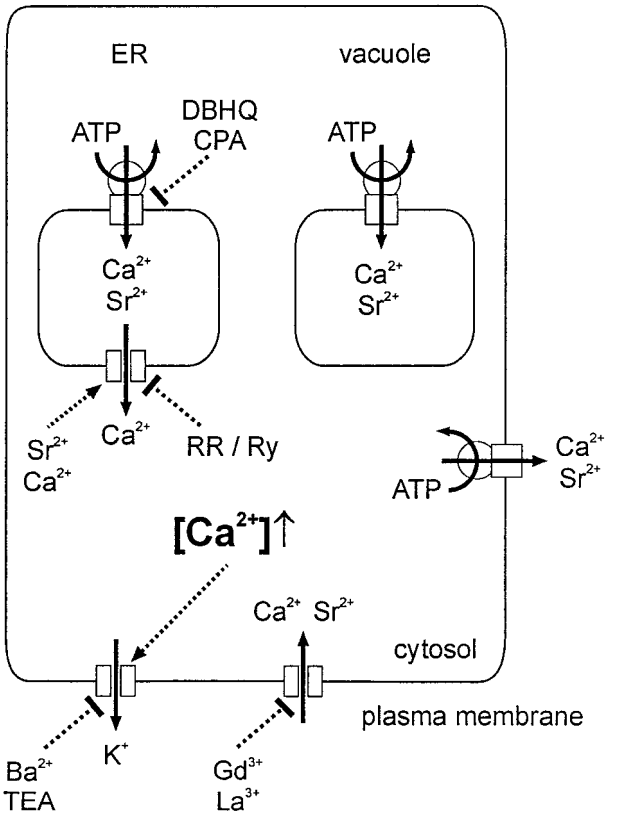

Figure 10. A schematic model for Sr^{2+}-induced $[Ca^{2+}]_{cy}$ spikes in *E. viridis*. Sr^{2+} enters the cell via Ca^{2+} channels in the plasma membrane that are competitively blocked by Gd^{3+} or La^{3+}. Most of the Sr^{2+} taken up into the cell is compartmentalized into the vacuole. At steady state, the same amount of Sr^{2+} (and Ca^{2+}) that enters the cell is transported out of the cell by plasma membrane Ca^{2+}-ATPases. The Ca^{2+}-ATPases that pump Sr^{2+} (and Ca^{2+}) into the vacuole or out of the cell are not blocked by DBHQ or CPA. Inside the cell Sr^{2+} induces a Ca^{2+}-release from the ER. The ER Ca^{2+} channel is inhibited by either ruthenium red (RR) or ryanodine (Ry), pointing to a ryanodine/cADPR-like Ca^{2+} channel. The rapid increase in $[Ca^{2+}]_{cy}$ is compensated for by Ca^{2+}-ATPases of internal Ca^{2+} stores and the plasma membrane. The ER is refilled by Ca^{2+}-ATPases that are blocked by DBHQ or CPA. The $[Ca^{2+}]_{cy}$ spike causes the opening of plasma membrane K^+ channels, resulting in a transient hyperpolarization. This K^+ channel is known to be blocked by Ba^{2+} or TEA (Köhler et al., 1983; Thaler et al., 1989).

store and probably plays a key role in ion homeostasis and compartmentalization (see above). However, the $[Ca^{2+}]_{cy}$ oscillations described here are driven by a rather small internal Ca^{2+} store, probably the ER, and not the vacuole (Fig. 10). In good agreement, Plieth et al. (1998) recently demonstrated that the elevation in $[Ca^{2+}]_{cy}$ during action potentials in *Chara* sp. is neither caused by Ca^{2+} influx across the plasma membrane nor by Ca^{2+} release from the vacuole. A Ca^{2+} release from internal stores different from the vacuole gives rise to elevated $[Ca^{2+}]_{cy}$ (Plieth et al., 1998).

The Sr^{2+}-induced $[Ca^{2+}]_{cy}$ oscillations in the unicellular green alga *E. viridis* show a dose-dependent frequency increase (Table I). This suggests that in *E. viridis*, comparable to animal cells, $[Ca^{2+}]_{cy}$ oscillations might encode information about external stimuli by their frequency, mediating stimulus-specific reactions by Ca^{2+}-dependent signal transduction processes. It is likely that Sr^{2+}-induced repetitive $[Ca^{2+}]_{cy}$ spikes are initialized by a Sr^{2+}-induced Ca^{2+} release from the ER via a type of ryanodine/cADPR Ca^{2+} release channel. Our current working model of the different transmembrane Ca^{2+} fluxes and compartments involved in Sr^{2+}-induced $[Ca^{2+}]_{cy}$ oscillations in *E. viridis* is summarized in Figure 10.

ACKNOWLEDGMENTS

We thank Prof. Sattelmacher, Kiel, Germany, for his generous support and cooperation, and Mrs. F. Reisberg for analyses by ICP-AES.

Received December 29, 1997; accepted March 3, 1998.
Copyright Clearance Center: 0032–0889/98/117/0545/13.

LITERATURE CITED

Allen GJ, Muir SR, Sanders D (1995) Release of Ca^{2+} from individual plant vacuoles by both $InsP_3$ and cyclic ADP-ribose. Science **268:** 735–737

Bauer CS, Plieth C, Hansen U-P, Sattelmacher B, Simonis W, Schönknecht G (1997) Repetitive Ca^{2+} spikes in a unicellular green alga. FEBS Lett **405:** 390–393

Berridge MJ (1993) Inositol trisphosphate and calcium signalling. Nature **361:** 315–325

Berridge MJ (1997) The AM and FM of calcium signalling. Nature **386:** 759–760

Bethmann B, Thaler M, Simonis W, Schönknecht G (1995) Electrochemical potential gradients of H^+, K^+, Ca^{2+}, and Cl^- across the tonoplast of the green alga *Eremosphaera viridis*. Plant Physiol **109:** 1317–1326

Bootman MD, Berridge MJ (1995) The elemental principles of calcium signaling. Cell **83:** 675–678

Bos-Mikich A, Swann K, Whittingham DG (1995) Calcium oscillations and protein synthesis inhibition synergistically activate mouse oocytes. Mol Reprod Dev **41:** 84–90

Busch MB, Sievers A (1993) Membrane traffic from the endoplasmic reticulum to the Golgi apparatus is disturbed by an inhibitor of the Ca^{2+}-ATPase in the ER. Protoplasma **177:** 23–31

Bush DS (1995) Calcium regulation in plant cells and its role in signaling. Annu Rev Plant Physiol Plant Mol Biol **46:** 95–122

Clapham DE (1995) Calcium signaling. Cell **80:** 259–268

D'Andrea P, Thorn P (1996) Ca^{2+} signalling in rat chromaffin cells: interplay between Ca^{2+} release from intracellular stores and membrane potential. Cell Calcium **19:** 113–123

De Koninck P, Schulman H (1998) Sensitivity of CaM kinase II to the frequency of Ca^{2+} oscillations. Science **279:** 227–230

Demaurex N, Lew DP, Krause K-H (1992) Cyclopiazonic acid depletes intracellular Ca^{2+} stores and activates an influx pathway for divalent cations in HL-60 cells. J Biol Chem **267:** 2318–2324

Du GG, Ashley CC, Lea TJ (1994) Effects of thapsigargin and cyclopiazonic acid on the sarcoplasmic reticulum Ca^{2+} pump of skinned fibres from frog skeletal muscle. Pflügers Arch **429:** 169–175

Ehrhardt DW, Wais R, Long SR (1996) Calcium spiking in plant root hairs responding to Rhizobium nodulation signals. Cell **85:** 673–681

Ehrlich BE, Kaftan E, Bezprozvannaya S, Bezprozvanny I (1994) The pharmacology of intracellular Ca^{2+}-release channels. Trends Pharmacol Sci **15:** 145–149

Felle H (1988) Auxin causes oscillations of cytosolic free calcium and pH in *Zea mays* coleoptiles. Planta **174:** 495–499

Fenton JM, Crofts AR (1990) Computer aided fluorescence imaging of photosynthetic systems: application of video imaging to the study of fluorescence induction of green plants and photosynthetic bacteria. Photosynth Res **26:** 59–66

Fewtrell C (1993) Ca^{2+} oscillations in non-excitable cells. Annu Rev Physiol **55:** 427–454

Förster B (1990) Injected inositol 1,4,5-trisphosphate activates Ca^{2+}-sensitive K^+ channels in the plasmalemma of *Eremosphaera viridis*. FEBS Lett **269:** 197–201

Grégoire G, Loirand G, Pacaud P (1993) Ca^{2+} and Sr^{2+} entry induced Ca^{2+} release from the intracellular Ca^{2+} store in smooth muscle cells of rat portal vein. J Physiol **474:** 483–500

Grynkiewicz G, Poenie M, Tsien RY (1985) A new generation of Ca^{2+} indicators with greatly improved fluorescent properties. J Biol Chem **260:** 3440–3450

Hajnóczky G, Robb-Gaspers LD, Seitz MB, Thomas AP (1995) Decoding of cytosolic calcium oscillations in the mitochondria. Cell **82:** 415–424

Huang JW, Grunes DL, Kochian LV (1994) Voltage-dependent Ca^{2+} influx into right-side-out plasma membrane vesicles isolated from wheat roots: characterization of a putative Ca^{2+} channel. Proc Natl Acad Sci USA **91:** 3473–3477

Hwang I, Ratterman DM, Sze H (1997) Distinction between endoplasmic reticulum-type and plasma membrane-type Ca^{2+} pumps. Partial purification of a 120-kilodalton Ca^{2+}-ATPase from endomembranes. Plant Physiol **113:** 535–548

Inesi G, Sagara Y (1994) Specific inhibitors of intracellular Ca^{2+} transport ATPases. J Membr Biol **141:** 1–6

Johannes E, Brosnan JM, Sanders D (1992) Parallel pathways for intracellular Ca^{2+} release from the vacuole of higher plants. Plant J **2:** 97–102

Johnson CH, Knight MR, Kondo T, Masson P, Sedbrook J, Haley A, Trewavas A (1995) Circadian oscillations of cytosolic and chloroplastic free calcium in plants. Science **269:** 1863–1865

Kass GEN, Duddy SK, Moore GA, Orrenius S (1989) 2,5-Di-(*tert*-butyl)-1,4-benzohydroquinone rapidly elevates cytosolic Ca^{2+} concentration by mobilizing the inositol 1,4,5-trisphosphate-sensitive Ca^{2+} pool. J Biol Chem **264:** 15192–15198

Klüsener B, Boheim G, Liss H, Engelberth J, Weiler EW (1995) Gadolinium-sensitive, voltage-dependent calcium release channels in the endoplasmic reticulum of a higher plant mechanoreceptor organ. EMBO J **14:** 2708–2714

Knight MR, Campbell AK, Smith SM, Trewavas AJ (1991) Transgenic plant aequorin reports the effect of touch and cold-shock and elicitors on cytoplasmic calcium. Nature **352:** 524–526

Knight MR, Smith SM, Trewavas AJ (1992) Wind-induced plant motion immediately increases cytosolic calcium. Proc Natl Acad Sci USA **89:** 4967–4971

Köhler K, Geisweid H-J, Simonis W, Urbach W (1983) Changes in membrane potential and resistance caused by transient increase of potassium conductance in the unicellular alga *Eremosphaera viridis*. Planta **159:** 165–171

Kwan C-Y, Putney JW, Jr (1990) Uptake and intracellular sequestration of divalent cations in resting and methacholine-stimulated mouse lacrimal acinar cells: dissociation by Sr^{2+} and Ba^{2+} of agonist-stimulated divalent cation entry from the refilling of the agonist-sensitive intracellular pool. J Biol Chem **265:** 678–684

Larsson O, Kindmark H, Bränström R, Fredholm B, Berggren PO (1996) Oscillations in K_{ATP} channel activity promote oscillations in cytoplasmic free Ca^{2+} concentration in the pancreatic β cell. Proc Natl Acad Sci USA **93:** 5161–5165

Lee HC, Aarhus R, Graeff RM (1995) Sensitization of calcium-induced calcium release by cyclic ADP-ribose and calmodulin. J Biol Chem **270:** 9060–9066

Lee SH, Earm YE (1994) Caffeine induces periodic oscillations of Ca^{2+}-activated K^+ current in pulmonary arterial smooth muscle cells. Pflügers Arch **426:** 189–198

Li YX, Keizer J, Stojilkovic SS, Rinzel J (1995a) Ca^{2+} excitability of the ER membrane: an explanation for IP_3-induced Ca^{2+} oscillations. Am J Physiol Cell Physiol **38:** C1079–C1092

Li YX, Rinzel J, Vergara L, Stojilkovic SS (1995b) Spontaneous electrical and calcium oscillations in unstimulated pituitary gonadotrophs. Biophys J **69:** 785–795

Liang F, Cunningham KW, Harper JF, Sze H (1997) ECA1 complements yeast mutants defective in Ca^{2+} pumps and encodes an endoplasmic reticulum-type Ca^{2+}-ATPase in *Arabidopsis thaliana*. Proc Natl Acad Sci USA **94:** 8579–8584

Logan DC, Venis MA (1995) Characterisation and immunological identification of a calmodulin-stimulated Ca^{2+}-ATPase from maize shoots. J Plant Physiol **145:** 702–710

Ma J (1993) Block by ruthenium red of the ryanodine-activated calcium release channel of skeletal muscle. J Gen Physiol **102:** 1031–1056

Marshall J, Corzo A, Leigh RA, Sanders D (1994) Membrane potential-dependent calcium transport in right-side-out plasma membrane vesicles from *Zea mays* L. roots. Plant J **5:** 683–694

McAinsh MR, Webb AAR, Taylor JE, Hetherington AM (1995) Stimulus-induced oscillations in guard cell cytosolic free calcium. Plant Cell **7:** 1207–1219

Meissner G (1994) Ryanodine receptor/Ca^{2+} release channels and their regulation by endogenous effectors. Annu Rev Physiol **56:** 485–508

Mironov SL, Juri MU (1990) Sr and Ba transients in isolated snail neurones studied with fura-2: the recovery from depolarization induced load and modulation of Ca release from intracellular stores. Neurosci Lett **112:** 184–189

Muir SR, Sanders D (1996) Pharmacology of Ca^{2+} release from red beet microsomes suggests the presence of ryanodine receptor homologs in higher plants. FEBS Lett **395:** 39–42

Pantoja O, Gelli A, Blumwald E (1992) Voltage-dependent calcium channels in plant vacuoles. Science **255:** 1567–1570

Petersen OH, Petersen CCH, Kasai H (1994) Calcium and hormone action. Annu Rev Physiol **56:** 297–319

Piñeros M, Tester M (1995) Characterization of a voltage-dependent Ca^{2+}-selective channel from wheat roots. Planta **195:** 478–488

Plieth C, Hansen U-P (1996) Methodological aspects of pressure loading of fura-2 into Characean cells. J Exp Bot **47:** 1601–1612

Plieth C, Sattelmacher B, Hansen U-P, Thiel G (1998) The action potential in *Chara*: Ca^{2+} release from internal stores visualized by Mn^{2+}-induced quenching of fura-dextran. Plant J **13:** 167–175

Rengel Z (1994) Effects of Al^{3+}, rare earth elements, and other metals on net $^{45}Ca^{2+}$ uptake by *Amaranthus* protoplasts. J Plant Physiol **143:** 47–51

Sauer G, Simonis W, Schönknecht G (1993) An inwardly rectifying cation current across the plasma membrane of the green alga *Eremosphaera viridis*. Plant Cell Physiol **34:** 1275–1282

Sauer G, Simonis W, Schönknecht G (1994) Divalent cation and anion currents are activated during the dark-induced transient hyperpolarization of the plasma membrane of the green alga *Eremosphaera viridis*. J Exp Bot **45:** 1403–1412

Schönknecht G, Bauer CS, Simonis W (1998) Light-dependent signal transduction and transient changes in cytosolic Ca^{2+} in a unicellular green alga. J Exp Bot **49:** 1–11

Schroeder JI, Hagiwara S (1990) Repetitive increases in cytosolic Ca^{2+} of guard cells by abscisic acid activation of nonselective Ca^{2+} permeable channels. Proc Natl Acad Sci USA **87:** 9305–9309

Schumaker KS, Sze H (1987) Inositol 1,4,5-trisphosphate releases Ca^{2+} from vacuolar membrane vesicles of oat roots. J Biol Chem **262:** 3944–3946

Smith JS, Imagawa T, Ma J, Fill M, Campbell KP, Coronado R (1988) Purified ryanodine receptor from rabbit skeletal muscle is the calcium-release channel of sarcoplasmic reticulum. J Gen Physiol **92:** 1–26

Stucki JW, Somogyi R (1994) A dialogue on Ca^{2+} oscillations: an attempt to understand the essentials of mechanisms leading to hormone-induced intracellular Ca^{2+} oscillations in various kinds of cells on a theoretical level. Biochim Biophys Acta **1183:** 453–472

Thaler M, Simonis W, Schönknecht G (1992) Light-dependent changes of the cytoplasmic H^+ and Cl^- activity in the green alga *Eremosphaera viridis*. Plant Physiol **99:** 103–110

Thaler M, Steigner W, Förster B, Köhler K, Simonis W, Urbach W (1989) Calcium activation of potassium channels in the plasmalemma of *Eremosphaera viridis*. J Exp Bot **40:** 1195–1203

Thomas AP, Bird GSJ, Hajnóczky G, Robb-Gaspers LD, Putney JW (1996) Spatial and temporal aspects of cellular calcium signaling. FASEB J **10:** 1505–1517

Trebacz K, Busch MB, Hejnowicz Z, Sievers A (1996) Cyclopiazonic acid disturbs the regulation of cytosolic calcium when repetitive action potentials are evoked in *Dionaea* traps. Planta **198:** 623–626

Trewavas A, Read N, Campbell AK, Knight M (1996) Transduction of Ca^{2+} signals in plant cells and compartmentalization of the Ca^{2+} signal. Biochem Soc Trans **24:** 971–974

Tsien RW, Tsien RY (1990) Calcium channels, stores and oscillations. Annu Rev Cell Biol **6:** 715–760

Webb AAR, McAinsh MR, Taylor JE, Hetherington AM (1996) Calcium ions as intracellular second messengers in higher plants. Adv Bot Res **22:** 45–96

Weidinger M, Ruppel HG (1985) Ca^{2+}-requirement for a blue-light-induced chloroplast translocation in *Eremosphaera viridis*. Protoplasma **124:** 184–187

Wojnowski L, Schwab A, Hoyland J, Mason WT, Sibernagl S, Oberleithner H (1994) Cytoplasmic Ca^{2+} determines the rate of Ca^{2+} entry into Mardin-Darby canine kidney-focus (MDCK-f) cells. Pflügers Arch **426:** 95–100

Zhang GH, Melvin JE (1993) Inhibitors of the intracellular Ca^{2+} release mechanism prevent muscarinic-induced Ca^{2+} influx in rat sublingual mucous acini. FEBS Lett **327:** 1–6